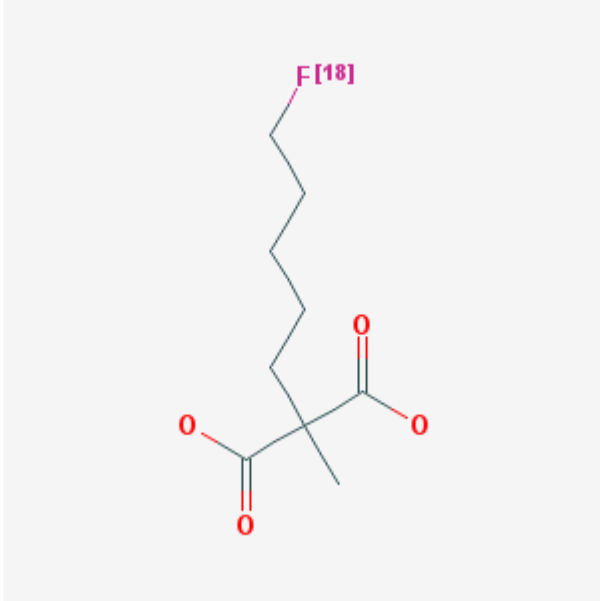


2-(5-[¹⁸F]Fluoro-pentyl)-2-methyl-malonic acid (ML-10)

[¹⁸F]ML-10

Arvind Chopra, PhD¹

Created: August 15, 2012; Updated: September 27, 2012.

Chemical name:	2-(5-[¹⁸ F]Fluoro-pentyl)-2-methyl-malonic acid (ML-10)	
Abbreviated name:	[¹⁸ F]ML-10	
Synonym:		
Agent Category:	Compound	
Target:	Apoptotic cells	
Target Category:	Other	
Method of detection:	Positron emission tomography (PET)	
Source of signal / contrast:	¹⁸ F	
Activation:	No	
Studies:	<ul style="list-style-type: none">• <i>In vitro</i>• Rodents• Humans	

Click on the above structure of 2-(5-[¹⁸F]fluoro-pentyl)-2-methyl-malonic acid (ML-10) for more information in [PubChem](#).

Background

[[PubMed](#)]

¹ National Center for Biotechnology Information, NLM, Bethesda, MD 20894; Email: micad@ncbi.nlm.nih.gov.

NLM Citation: Chopra A. 2-(5-[¹⁸F]Fluoro-pentyl)-2-methyl-malonic acid (ML-10). 2012 Aug 15 [Updated 2012 Sep 27]. In: Molecular Imaging and Contrast Agent Database (MICAD) [Internet]. Bethesda (MD): National Center for Biotechnology Information (US); 2004-2013.

Radiotherapy, chemotherapy, or a combination of the two are often used in the clinic to induce apoptosis, the process of programmed cell death, in cancerous tumor cells in order to treat neoplasms (1). Radiolabeled proteins, such as ^{99m}Tc - or ^{123}I -labeled annexin V and its derivatives that have a high affinity for externalized anionic phospholipids (e.g., phosphatidylserine (PS)) on apoptotic cells, were shown to be suitable for monitoring the efficacy and response to anticancer treatments with noninvasive imaging techniques such as single-photon emission tomography (2). In a preliminary study, it was shown that the ^{99m}Tc -labeled C2A domain of synaptaginin I (binds to PS) can also be used for the imaging of non-small cell lung cancer tumor apoptosis in mice (3). However, none of these tracers can be used to visualize the progression of cell death in neoplastic lesions because these probes either have a slow clearance rate and generate a low signal/noise ratio, have unsuitable biodistribution characteristics, or tend to be immunogenic (4). Hence, there is much interest to develop and evaluate imaging probes that can be used with various imaging modalities, such as positron emission tomography (PET), to observe the initiation and progress of cellular apoptosis under normal and pathological conditions (4).

Damianovich et al. reported the development of a group of small molecule compounds, classified as ApoSense, and showed that systemic administration of a fluorescent or radiolabeled compound resulted in a selective accumulation of the tracer in apoptotic cells in three animal models of human cancers (5). A characteristic feature of the ApoSense compounds is that they are not transported across the cell membrane but pass through the plasma membrane and accumulate within the cytoplasm of apoptotic cells after initiation of apoptosis (6). To see a video of this phenomenon, [click here](#). It was shown that two members of the ApoSense family, *N,N'*-didansyl-L-cystiene (DDC) (5) and 5-(dimethylamino)-1-naphthalenesulfonyl- α -ethyl- ^{18}F fluoroalanine (^{18}F]NST-732) (6), can be used for the *in vivo* imaging of apoptosis in rodents with fluorescence (DDC and ^{18}F]NST-732) and PET (^{18}F]NST-732) imaging techniques. In a continued effort to develop an ^{18}F -labeled compound that can be used for the visualization of apoptosis with PET in the clinic, a small molecule with only a few functional moieties, 2-(5- ^{18}F fluoro-pentyl)-2-methyl-malonic acid (^{18}F]ML-10), was synthesized and evaluated for the detection of apoptotic cells in a mouse model of cerebral stroke (7). The biodistribution of ^{18}F]ML-10 has been investigated in healthy rats (7) and healthy human volunteers (8). In another study, it was shown that ^{18}F]ML-10 can be used with PET to detect the early response of metastases in the brain to whole-brain radiation therapy (9).

Related Resource Links

Apoptosis related chapters in [MICAD](#)

[Clinical trials \(apoptosis\)](#)

[Apoptosis pathways](#)

Synthesis

[PubMed]

The synthesis and purification of $[^{18}\text{F}]$ ML-10 with high-performance liquid chromatography (HPLC) has been described by Reshef et al. (7). The radiochemical yield (RCY) of HPLC-purified $[^{18}\text{F}]$ ML-10 was 30%–40% at the end of synthesis, with a radiochemical purity (RCP) of >99% and a specific activity (SA) of >40.7 GBq/ μmol (1.505 Ci/ μmol). The total time required for the synthesis was ~75 min.

An automated method for the synthesis of $[^{18}\text{F}]$ ML-10 has been described by Sobrio et al. (10). The RCY of the labeled compound was $39.8 \pm 8.4\%$ ($n = 7$ reactions), with an RCP of >99% and a SA of 235 ± 85 GBq/ μmol (8.69 ± 3.14 Ci/ μmol). The synthesis of $[^{18}\text{F}]$ ML-10 was completed in 70 min.

^3H -Labeled ML-10 ($[^3\text{H}]$ ML-10) was synthesized for *in vitro* studies with Jurkat cells (a human T-cell leukemia cell line) as described elsewhere (7). Fluorescent dye-labeled dansyl-ML-10 was synthesized for the histopathological examination of tissues in some studies (8).

In Vitro Studies: Testing in Cells and Tissues

[PubMed]

The uptake of $[^3\text{H}]$ ML-10 was studied in Jurkat cells before apoptosis (control), after the induction of apoptosis (by exposure to anti-Fas antibody), and after the inhibition of apoptosis (by treatment with a caspase inhibitor) (7). Only cells undergoing apoptosis showed a significantly higher uptake ($P < 0.001$; ~9-fold) of radioactivity ($1.87 \pm 0.06\%$ of total added radioactivity (% TAR)) compared with the control cells ($0.20 \pm 0.01\%$ TAR) and the apoptosis-inhibited cells ($0.25 \pm 0.01\%$ TAR).

In another study, the uptake of $[^3\text{H}]$ ML-10 by necrotic cells (Jurkat cells; necrosis induced by freeze-thaw cycles) was compared with that of control cells (7). A similar accumulation of radioactivity was observed both in the control cells and the necrotic cells.

Results obtained from these studies indicated that $[^3\text{H}]$ ML-10 accumulated selectively in the apoptotic cells and can distinguish the apoptotic cells from the normal and the necrotic cells.

Animal Studies

Rodents

[PubMed]

The biodistribution of $[^{18}\text{F}]$ ML-10 was studied in healthy CD rats (7). The animals ($n = 5$ rats/time point) were given an intravenous injection (site not reported) of 0.37 MBq

(~13.7 μCi) [^{18}F]ML-10 and euthanized at time points ranging from 5 min postinjection (p.i.) to 240 min p.i. The various organs of interest were harvested from the rats to determine the amount of radioactivity that accumulated in the tissues. Results were presented as percent of injected dose per gram tissue (% ID/g). No specific organ in the animals was observed to accumulate the tracer. All organs except the kidneys showed an uptake of <1% ID/g at 5 min p.i., and this level decreased gradually for up to 240 min p.i. At 5 min p.i., the kidneys showed an accumulation of $2.7 \pm 0.88\%$ ID/g of the tracer, and this level decreased to $0.05 \pm 0.01\%$ ID/g by 240 min p.i. The circulation half-life of the radiochemical was reported to be 23 min. The investigators concluded that the biodistribution of [^{18}F]ML-10 in the rats was as expected because the labeled compound is not supposed to be taken up by healthy cells in tissues (7).

HPLC analysis of plasma and brain tissue obtained at 90 min p.i. from healthy rats injected with 50 MBq (1.85 mCi) [^{18}F]ML-10 showed that >97% of the radiochemical was intact (7). This indicated that an insignificant amount of the labeled compound was metabolized *in vivo*.

Dynamic small-animal PET images were acquired from mice (number of animals not reported) with cerebral ischemia (induced by middle cerebral artery occlusion; MCAO mice) 45–90 min after injection of 0.37 MBq (~13.7 μCi) [^{18}F]ML-10 (7). The images showed that the uptake of the tracer was multifocal, like a gradient, and was present only in the parenchyma of the cortical and subcortical regions of the affected left hemisphere of the brain. Very low levels of the tracer were evident in the unaffected contralateral cerebral hemisphere of the animals. Phosphorimaging and a histopathological examination of the brain sections obtained from MCAO mice injected with [^{18}F]ML-10 showed that there was a correlation between areas showing the presence of radioactivity and the cells that exhibited the characteristics of apoptosis (r^2 values not reported) (7).

In another study, male BALB/c mice (number not reported) were injected with 20 MBq (0.74 mCi) [^{18}F]ML-10, and the anesthetized mice were subject to a whole-body PET scan for 120 min (8). From the images it was apparent that the tracer accumulated primarily in the testes of the animals. Histopathological examination of the testes obtained from mice treated with dansyl-ML-10 showed that the tracer accumulated only in those sections of the organs with apoptotic cells.

Other Non-Primate Mammals

[PubMed]

No publications are currently available.

Non-Human Primates

[PubMed]

No publications are currently available.

Human Studies

[PubMed]

The biodistribution of $[^{18}\text{F}]$ ML-10 was studied in 8 healthy human volunteers (four men and four women (mean age range, 21–44 y; weight, 69 ± 11 kg)) (8). The individuals were given an intravenous injection of 233 ± 90 MBq (8.6 ± 3.3 mCi) $[^{18}\text{F}]$ ML-10, and whole-body PET/computed tomography (CT) scans were acquired from the subjects for up to 220 min p.i. as detailed by Hoglund et al. (8). The images showed that the tracer was cleared from all the non-target organs and excreted into the urinary bladder by 10 min p.i. The blood circulation half-life and the organ elimination half-life of the tracer were 1.3 ± 0.1 h and 1.1 ± 0.2 h, respectively. All male subjects showed an accumulation of the probe in the testes as reported with the male mice (see above). The accumulation of tracer in the testes peaked at ~25 min p.i., plateaued at ~90 min p.i., and showed a gradual decrease after this time point. The biodistribution profile of $[^{18}\text{F}]$ ML-10 was observed to be similar among all the male and female subjects enrolled in the study. From this study, the investigators concluded that, because $[^{18}\text{F}]$ ML-10 had a suitable biodistribution and safety profile in humans, it can be developed as a PET agent for the detection of apoptosis in the clinic (8).

The use of $[^{18}\text{F}]$ ML-10 was evaluated in 10 patients to assess the response of brain metastases to whole-brain radiation therapy (9). Each patient underwent a baseline PET scan (before initiation of radiation treatment) and a PET scan after radiotherapy (after 9 or 10 treatments). The amount of $[^{18}\text{F}]$ ML-10 administered to each participant did not exceed ~0.5 GBq (13.5 mCi). Magnetic resonance images (MRI) were acquired from each patient at 6–8 weeks after completion of the radiation treatment. In all patients, the brain lesions were detectable with both $[^{18}\text{F}]$ ML-10 PET and MRI scans. In addition, a high correlation was observed between the early changes noticed with PET scans and the alteration in tumor anatomical dimensions observed later with the MRI scans ($r = 0.9$). Only 9 patients completed the pre- and post-treatment $[^{18}\text{F}]$ ML-10 PET/CT scans (9). From the post-treatment scan images, the ratios of mean uptake of radioactivity in the lesion (signal) and the corresponding contralateral healthy brain tissues (background) were determined. The mean signal/background ratios for scans performed at 20–36 min p.i., 80–100 min p.i., and 130–150 min p.i. were 4.62 ± 2.64 , 6.63 ± 3.81 , and 8.76 ± 5.59 , respectively. This indicated that the tracer accumulated in the cancerous lesions over time but was cleared rapidly from the noncancerous areas of the brain. From this study, the investigators concluded that $[^{18}\text{F}]$ ML-10 was probably suitable to determine tumor responsiveness to anticancer therapy in humans (9).

In another study $[^{18}\text{F}]$ ML-10 was used for the imaging of apoptotic neurovascular cells in patients with acute ischemic cerebral stroke (11).

Supplemental Information

[Disclaimers]

No information is currently available.

References

1. Haimovitz-Friedman A., Yang T.I., Thin T.H., Verheij M. *Imaging radiotherapy-induced apoptosis*. Radiat Res. 2012;177(4):467–82. PubMed PMID: 22348249.
2. De Saint-Hubert M., Bauwens M., Verbruggen A., Mottaghy F.M. *Apoptosis imaging to monitor cancer therapy: the road to fast treatment evaluation?* Curr Pharm Biotechnol. 2012;13(4):571–83. PubMed PMID: 22214506.
3. Wang F., Fang W., Zhao M., Wang Z., Ji S., Li Y., Zheng Y. *Imaging paclitaxel (chemotherapy)-induced tumor apoptosis with ^{99m}Tc C2A, a domain of synaptotagmin I: a preliminary study*. Nucl Med Biol. 2008;35(3):359–64. PubMed PMID: 18355692.
4. Cohen A., Shirvan A., Levin G., Grimberg H., Reshef A., Ziv I. *From the Gla domain to a novel small-molecule detector of apoptosis*. Cell Res. 2009;19(5):625–37. PubMed PMID: 19223854.
5. Damianovich M., Ziv I., Heyman S.N., Rosen S., Shina A., Kidron D., Aloya T., Grimberg H., Levin G., Reshef A., Bentolila A., Cohen A., Shirvan A. *ApoSense: a novel technology for functional molecular imaging of cell death in models of acute renal tubular necrosis*. Eur J Nucl Med Mol Imaging. 2006;33(3):281–91. PubMed PMID: 16317537.
6. Aloya R., Shirvan A., Grimberg H., Reshef A., Levin G., Kidron D., Cohen A., Ziv I. *Molecular imaging of cell death in vivo by a novel small molecule probe*. Apoptosis. 2006;11(12):2089–101. PubMed PMID: 17051335.
7. Reshef A., Shirvan A., Waterhouse R.N., Grimberg H., Levin G., Cohen A., Ulysse L.G., Friedman G., Antoni G., Ziv I. *Molecular imaging of neurovascular cell death in experimental cerebral stroke by PET*. J Nucl Med. 2008;49(9):1520–8. PubMed PMID: 18703595.
8. Høglund J., Shirvan A., Antoni G., Gustavsson S.A., Langstrom B., Ringheim A., Sorensen J., Ben-Ami M., Ziv I. *^{18}F -ML-10, a PET tracer for apoptosis: first human study*. J Nucl Med. 2011;52(5):720–5. PubMed PMID: 21498526.
9. Allen A.M., Ben-Ami M., Reshef A., Steinmetz A., Kundel Y., Inbar E., Djaldetti R., Davidson T., Fenig E., Ziv I. *Assessment of response of brain metastases to radiotherapy by PET imaging of apoptosis with $(^{18}\text{F})\text{-ML-10}$* . Eur J Nucl Med Mol Imaging. 2012;39(9):1400–8. PubMed PMID: 22699524.
10. Sobrio, F., M. Medoc, L. Martial, J. Delamare, and L. Barre, *Automated Radiosynthesis of $[(^{18}\text{F})\text{ML-10}]$, a PET Radiotracer Dedicated to Apoptosis Imaging, on a TRACERLab FX-FN Module*. Mol Imaging Biol, 2012
11. Reshef A., Shirvan A., Akselrod-Ballin A., Wall A., Ziv I. *Small-molecule biomarkers for clinical PET imaging of apoptosis*. J Nucl Med. 2010;51(6):837–40. PubMed PMID: 20484422.